

# Dust Disks Around Young Stellar Objects

Kyung-Won Suh<sup>†</sup>

Department of Astronomy and Space Science, Chungbuk National University, Cheongju 28644, Korea

To reproduce the spectral energy distributions (SEDs) of young stellar objects (YSOs), we perform radiative transfer model calculations for the circumstellar dust disks with various shapes and many dust species. For eight sample objects of T Tauri and Herbig Ae/Be stars, we compare the theoretical model SEDs with the observed SEDs described by the infrared space observatory and Spitzer space telescope spectral data. We use the model, CGPLUS, for a passive irradiated circumstellar dust disk with an inner hole and an inner rim for the eight sample YSOs. We present model parameters for the dust disk, which reproduce the observed SEDs. We find that the model requires a higher mass, luminosity, and temperature for the central star for the Herbig Ae/Be stars than those for the T Tauri stars. Generally, the outer radius, total mass, thickness, and rim height of the theoretical dust disk for the Herbig Ae/Be stars are larger than those for the T Tauri stars.

**Keywords:** stars: pre-main sequences, infrared: stars, circumstellar matter, dust: extinction

## 1. INTRODUCTION

Young stellar objects (YSOs) are surrounded by a gas and dust disk as a consequence of the star formation process (e.g., Hartmann 2009). The T Tauri stars are generally known to be low-mass ( $0.1-2 M_{\text{sun}}$ ) pre-main sequence (PMS) stars. The Classical T Tauri (CTT) stars are optically visible because they have relatively thinner dust envelopes (e.g., Bertout 1989). The Herbig Ae/Be (HAB) stars are generally believed to be intermediate-mass ( $2-10 M_{\text{sun}}$ ) PMS stars (e.g., Waters & Waelkens 1998).

To understand the physical and chemical properties of the circumstellar disk, high-resolution infrared (IR) spectral observations are required. The infrared space observatory (ISO) and Spitzer space telescope (Spitzer) have provided high resolution spectroscopic observational data revealing detailed spectral energy distributions (SEDs) of many YSOs, which show various amorphous and crystalline dust features (Meeus et al. 2001; Olofsson et al. 2009; Sicilia-Aguilar et al. 2009).

In this study, we present theoretical models for the circumstellar dust disks around eight sample YSOs (four

CTT stars and four HAB stars) using the opacity functions of various amorphous and crystalline dust species. We use the radiative transfer model, CGPLUS, for the irradiated circumstellar dust disks developed by Dullemond et al. (2001). Even though this model uses a single dust component of the disk geometry ignoring dust shell components, it is useful for investigating the overall properties of the disk around the central star. We compare the model SEDs with the observed SEDs for the sample stars and obtain the theoretical model parameters that reproduce the observed SEDs.

## 2. SAMPLE STARS

In two previous studies (Suh 2011; Suh & Kwon 2011; hereafter SK2011), a radiative transfer model for multiple isothermal circumstellar dust shells was used to reproduce the observed SEDs for eight CTT stars and eight HAB stars. In this work, we choose four CTT stars and four HAB stars that can be more easily fitted by the model for a single dust disk, which is used in this work (see section 3). This better fit could be because the contribution from the dust shell

© This is an Open Access article distributed under the terms of the Creative Commons Attribution Non-Commercial License (<http://creativecommons.org/licenses/by-nc/3.0/>) which permits unrestricted non-commercial use, distribution, and reproduction in any medium, provided the original work is properly cited.

Received Mar 17, 2016 Revised Apr 28, 2016 Accepted Apr 29, 2016

<sup>†</sup>Corresponding Author

E-mail: kwsuh@chungbuk.ac.kr, ORCID: 0000-0001-9104-9763  
Tel: +82-43-261-2315, Fax: +82-43-274-2312

components is relatively small compared to the contribution from the dust disk for the new eight sample stars.

For the eight sample stars listed in Table 1, good quality observational data, including the Spitzer or ISO spectral data in a wide wavelength range, are available. We use the Spitzer infrared spectrograph (IRS) data for the CTT stars (Olofsson et al. 2009; Sicilia-Aguilar et al. 2009). For the HAB stars, we use the ISO short wavelength spectrometer (SWS) ( $\lambda = 2.4\text{-}45.2 \mu\text{m}$ ) and long wavelength spectrometer (LWS) ( $\lambda = 43\text{-}197 \text{mm}$ ) data reduced by Meeus et al. (2001).

For the sample stars, we use the data from the AKARI (Murakami et al. 2007) point source catalog (PSC) and

Bright Source Catalog (BSC) data in six bands (9, 18, 65, 90, 140, and 160  $\mu\text{m}$ ). We use the PSC data from the two micron all sky survey (2MASS) (Skrutskie et al. 2006) in 1.25, 1.65, and 2.17  $\mu\text{m}$  bands. We use the wide-field infrared survey explorer (WISE) (Wright et al. 2010) data in four bands (3.4, 4.6, 12, and 22  $\mu\text{m}$ ). We also use the ground-based infrared observational data obtained from various authors.

For each object, Table 1 lists the infrared astronomical satellite (IRAS) PSC, AKARI PSC, AKARI BSC numbers, and the model parameters for the central star (see section 3.3). In Figs. 1 and 2, we present the observed SEDs of the eight sample stars compared with the theoretical model SEDs (see section 3).

**Table 1.** Sample of the YSOs and the model parameters for the central star

Type	Name	IRAS PSC	AKARI PSC	AKARI BSC	$M_{\text{star}}$ ( $M_{\text{sun}}$ )	$L_{\text{star}}$ ( $L_{\text{sun}}$ )	$T_{\text{eff}}$ (K)	D (pc)
CTT	Haro 1-16	16285-2421	1631334-242737	1631337-242734	0.30	1.5	3,500	187
CTT	VW Cha	-	1108012-774229	-	0.04	1.8	3,000	155
CTT	WX Cha	11085-7720	1109586-773708	1107526-774234	0.25	0.7	2,600	157
CTT	J0843	08450-7854	0843184-790517	-	0.30	0.13	3,000	97
HAB	AB Aur	04525+3028	0455458+303303	0455460+303320	2.5	47	9,750	144
HAB	HD 100546	11312-6955	1133254-701140	113251-701140	2.5	37	11,000	103
HAB	HD 144432	16038-2735	1606579-274310	1606579-274308	2.2	32	8,000	200
HAB	HD 150193	16372-2347	-	1640176-235344	2.6	40	10,000	150

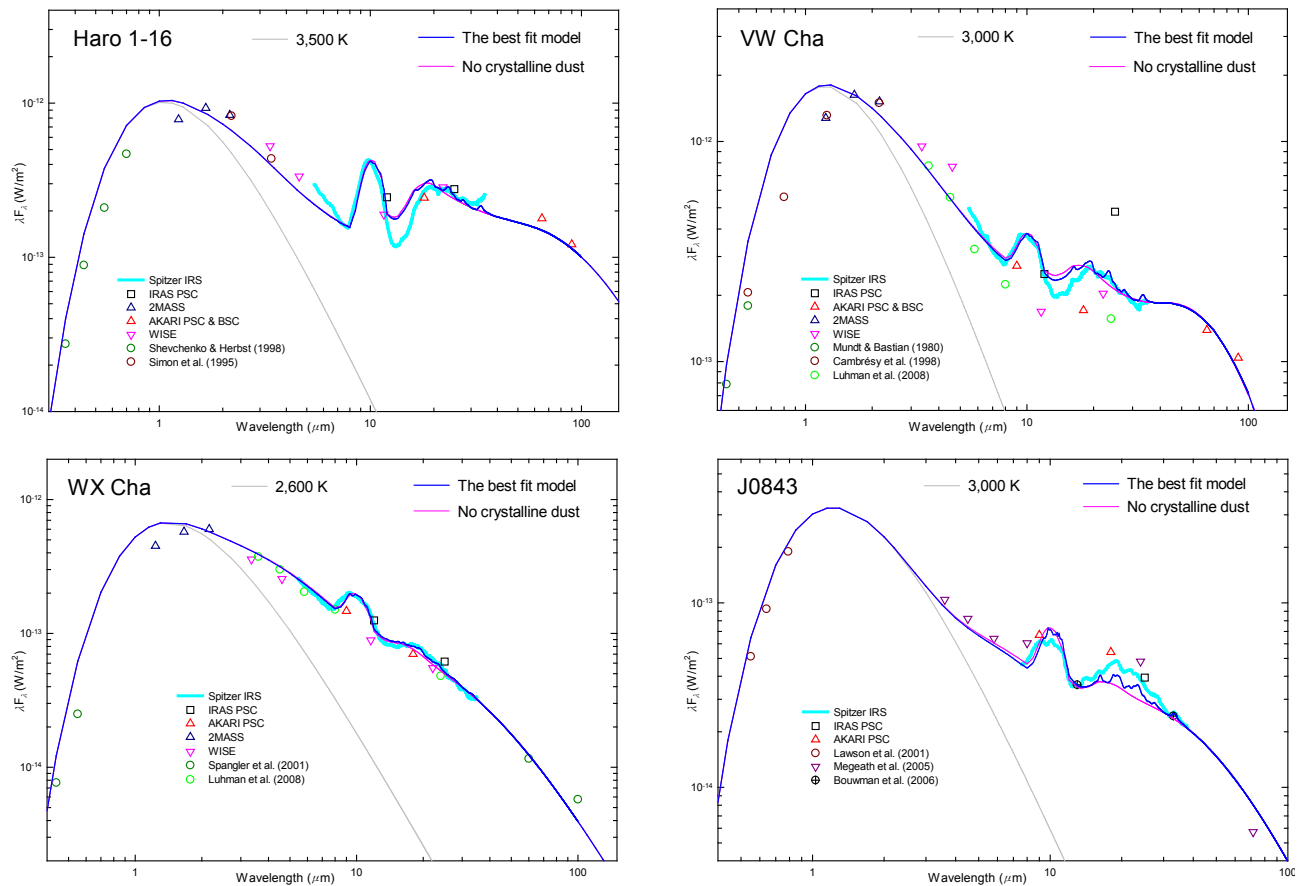


**Fig. 1.** Observations compared with the model SEDs for the sample CTT stars.

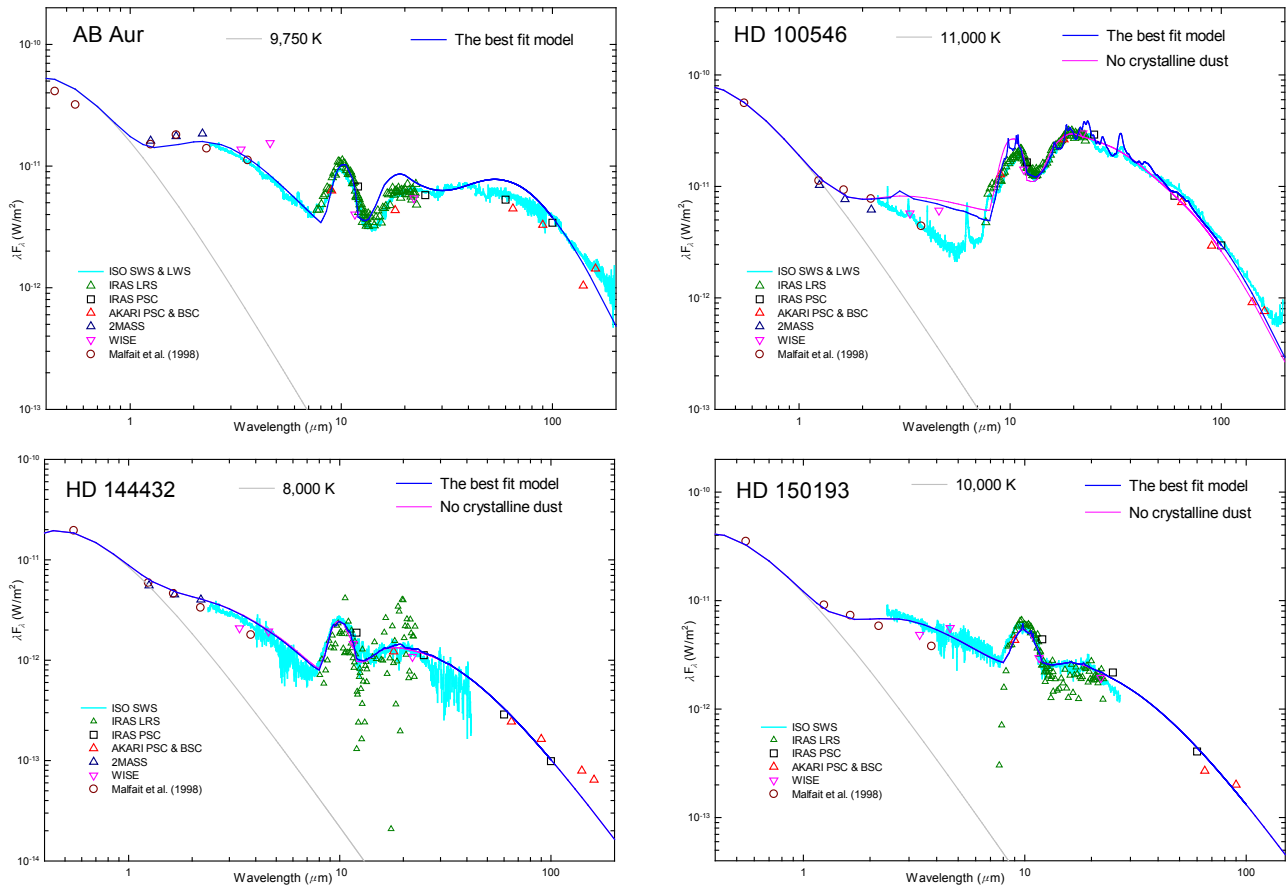


Fig. 2. Observations compared with the model SEDs for the sample HAB stars.

### 3. DUST DISK MODEL CALCULATIONS

The observed SEDs of YSOs were reproduced by using various models. Using a simple Planck dust radiation law, Bouwman et al. (2008) and Olofsson et al. (2010) tried to reproduce the observed SEDs of the YSOs. To overcome the limitation of the single component dust shell model (e.g., DUSTY developed by Ivezić & Elitzur 1997), SK2011 used a radiative transfer model for the multiple isothermal circumstellar dust shells to reproduce the observed SEDs of the YSOs. However, the dust envelopes of the YSOs are believed to have a disk geometry (e.g., Whitney et al. 2003).

#### 3.1 The Radiative Transfer Model

In this work, we perform the radiative transfer model calculations using the CGPLUS model developed by Dullemond et al. (2001) for a passive irradiated circumstellar dust disk to reproduce the observed SEDs of the sample YSOs. The model is based on the flaring disk model given by Chiang & Goldreich (1997). However, the central regions of

the disk are removed, and the inner rim of the disk is puffed up and is much hotter than the rest of the disk because it is directly exposed to the stellar flux. The circumstellar dust disk with an inner hole is irradiated and flared by the central star. The model can use various parameters of the disk geometry to consider radiative processes through the dust disk, but does not consider the scattering processes by dust or absorption processes by molecules. We model the dust disks around the YSOs using the opacity functions of various dust species (see section 3.2).

The dust density distribution uses a simple power law with a power law index ( $\alpha$ ) in the radial direction. The disk is almost isothermal in the vertical direction, leading to a Gaussian density distribution with a constant pressure scale height ( $h_{cg}$ ), which is a function of the isothermal temperature, central star parameters, and radial distance (Dullemond et al. 2001). The ratio of the disk surface height ( $h_{cg}$ ) to the pressure scale height ( $h_{cg}$ ) is a dimensionless number  $\chi_{cg}$  of order unity  $H_{cg} = \chi_{cg} h_{cg}$ . Generally, the disk with a larger  $\chi_{cg}$  is flared to a greater extent (or thicker).

The disk has six adjustable input parameters: the outer

radius ( $R_{out}$ ), total disk mass ( $M_{disk}$ ) assuming a gas-to-dust ratio of 100, power law index ( $\alpha$ ), dust temperature ( $T_{in}$ ) at the inner radius ( $R_{in}$ ),  $\chi_{cg}$ , and inclination angle ( $i$ ). Table 2 lists the model parameters of the dust disk for the best fit model (see section 3.3). The model calculates two derived parameters of the disk shape ( $R_{in}$  and the rim height,  $H_{rim}$ ), the dust temperature distribution including the dust temperature ( $T_{out}$ ) at the outer radius of the disk ( $R_{out}$ ), and the model SED. Though the CGPLUS model is relatively simple, using a single component dust disk, it is useful for deriving the physical parameters of the dust disk.

For the central hot source, we assume that the object is a single star that emits simple blackbody radiation. The model parameters for the central star are the mass, luminosity, blackbody temperature, and distance ( $D$ ).

### 3.2 Dust Opacity

Dust grains in the disk of the YSOs absorb and scatter the stellar radiation and re-emit the radiation at longer wavelengths. In this work, we use the seven dust species listed in Table 3. We do not consider the polycyclic aromatic hydrocarbons (PAH).

For amorphous dust, we use two dust species: amorphous silicate and amorphous carbon (AMC). We use the optical constants derived by Suh (1999) for amorphous warm silicate. We use the optical constants derived by Suh (2000) for AMC. For crystalline olivine and water-ice, we use the optical constants obtained by Fabian et al. (2001) and those obtained by Bertie et al. (1969), respectively.

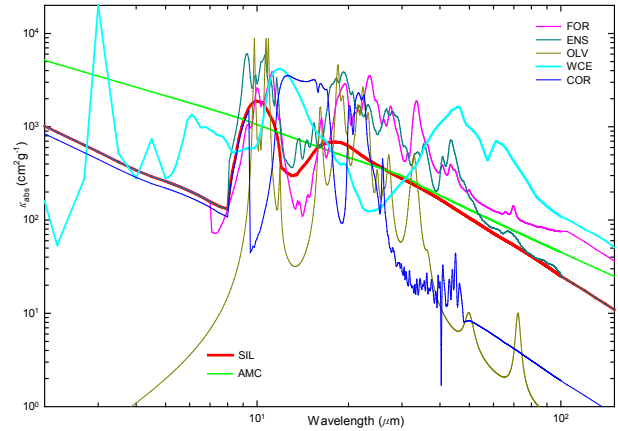


Fig. 3. Dust opacity functions used for this work (see Table 3).

For crystalline corundum, we use the optical constants of  $\alpha\text{-Al}_2\text{O}_3$  (corundum-sample 1) obtained by Tamanai et al. (2009). For the five dust species, we calculate the mass absorption coefficients (MACs) using the Mie theory (Bohren & Huffman 1983) from the optical constants. The uniform radius of the spherical dust grains is assumed to be 0.1  $\mu\text{m}$ .

For crystalline forsterite and enstatite, the MAC data obtained by Jäger et al. (1998) are used. Dust opacity functions for the seven species are displayed in Fig. 3. The crystalline dust grains show conspicuous emission features.

### 3.3 Model SEDs

We perform model calculations (see section 3.1) in the wavelength range from 0.1 to 200  $\mu\text{m}$ . We find a set of model

Table 2. Model parameters of the dust disk for the best fit model

Name	$R_{out}$ (AU)	$M_{disk}$ ( $M_{sun}$ )	$\alpha$	$T_{in}$ (K)	$\chi_{cg}$	$R_{in}$ (AU)	$T_{out}$ (K)	$H_{rim}$ (AU)	$i$ ( $^\circ$ )	Dust opacity <sup>1</sup>
Haro 1-16	30	8.0E-3	-0.8	1,400	3.0	0.137	105	0.014	50	0.9s+0.05a+0.05f
VW Cha	30	3.0E-4	-1.1	1,200	2.2	0.123	124	0.019	65	0.4s+0.55a+0.05f
WX Cha	2.0	1.0E-2	-2.5	900	3.5	0.174	256	0.034	60	0.7s+0.15a+0.07f+0.05e+0.03c
J0843	1.5	3.0E-3	2.2	600	1.8	0.161	216	0.014	60	0.58s+0.25a+0.12f+0.02o+0.03c
AB Aur	300	5.0E-2	-1.8	1,500	5.5	0.518	110	0.10	60	0.9s+0.1a
HD 100546	600	1.0E-2	0.5	1,200	1.2	0.671	83.0	0.029	55	0.6s+0.14a+0.11f+0.08o+0.02w+0.05c
HD 144432	10	5.0E-2	0.5	1,500	4.5	0.425	383	0.061	40	0.8s+0.03a+0.1f+0.05e+0.02c
HD 150193	10	5.0E-2	-0.5	1,300	2.2	0.604	460	0.064	63	0.85s+0.1a+0.05o

<sup>1</sup>s: SIL, a: AMC, f: FOR, e: ENS, o: OL, w: WIC, c: COR (See Table 3)

Table 3. Dust opacity functions used in this work

Acronym	Dust	Wavelength range ( $\mu\text{m}$ )	Size ( $\mu\text{m}$ )	Density ( $\text{g cm}^{-3}$ )	Reference
SIL	Amorphous warm silicate	0.01 ~ 36,000	0.1	3.3	Suh (1999)
AMC	Amorphous carbon	0.01 ~ 36,000	0.1	2.0	Suh (2000)
FOR	Crystalline forsterite	7.1 ~ 100	MAC	-	Jäger (1998)
ENS	Crystalline enstatite	8.1 ~ 99.5	MAC	-	Jäger (1998)
OLV	Crystalline olivine	9.78 ~ 72.5	0.1	3.3	Fabian et al. (2001)
WCE	Crystalline water-ice	2.5 ~ 333.3	0.1	0.92	Bertie et al. (1969)
COR	Crystalline corundum	21.1 ~ 1,000	0.1	4.0	Tamanai et al. (2009)

parameters that produces a similar fit to the observed SED and revise the related parameter ( $s$ ) to find a model with better fit in a wide wavelength range. At some point in this revision process, we find the best fit model, as it would not be possible to find a better model because of the limitation of the theoretical model, which uses a single dust disk component.

The best fit model SEDs are presented in Figs. 1 and 2. We list the model parameters of the central star and dust disk for the best fit models in Tables 1 and 2. Table 1 lists the model parameters of the central star: the mass ( $M_{star}$ ), luminosity ( $L_{star}$ ), effective blackbody temperature ( $T_{eff}$ ), and distance ( $D$ ) for each object. Table 2 lists the model parameters of the dust disk,  $R_{out}$ ,  $M_{disk}$ ,  $\alpha$ ,  $T_{in}$ ,  $\chi_{cg}$ ,  $R_{in}$ ,  $T_{out}$ ,  $H_{rim}$ ,  $i$  ( $i = 90^\circ$  for the edge on view), and dust opacity. The meanings of the model parameters are explained in section 3.1. For dust opacity, we list the dust composition, which is a simple mixture of dust species (see section 3.2) by mass.

#### 4. COMPARISON OF THE SEDS

Figs. 1 and 2 display the best fit theoretical model SEDs as well as the observed SEDs for the four CTT and four HAB sample stars. The theoretical model reproduces the observed SEDs, including the fine spectral features using crystalline dust as well as amorphous dust in the disk for most of the sample stars. The model SEDs, which do not use the crystalline dust, are also shown for comparison. When crystalline dust is not used,  $M_{disk}$  decreases by 5–26% depending on the crystalline dust content (see Table 2), the temperature distribution changes slightly, the optical depths at some wavelengths become significantly smaller, and the crystalline features are suppressed.

Haro 1-16 appears to have very abundant (90%) silicate dust, and it shows prominent 10 and 20  $\mu\text{m}$  features. The object seems to have a relatively hotter (3,500K) central star compared with the other CTT objects. The forsterite features at 23.5, 27.5, and 33.5  $\mu\text{m}$  are reproduced by the model. Because of the limitation of the theoretical model, which uses a single disk component, the model fit in some wavelength ranges could not be improved.

For VW Cha, the crystalline forsterite features are reproduced by the best fit model, which requires the highest AMC content (55%). This object appears to have the smallest disk mass ( $3 \times 10^{-4} M_{sun}$ ).

For WX Cha, the crystalline features could be due to various crystalline dust species (forsterite, enstatite, and corundum). The model requires the largest disk mass ( $1 \times 10^{-2} M_{sun}$ ) among the four sample CTT stars.

J0843 appears to be the nearest ( $D = 97$  pc) object for which the model requires the lowest stellar luminosity ( $0.13 L_{sun}$ ) and detached dust disk ( $T_{in} = 600\text{K}$ ). The object shows weak crystalline dust features due to various crystalline dust species (forsterite, olivine, and corundum) and some unknown features.

For AB Aur, the model uses only amorphous dust (silicate and AMC). Unlike the other objects, the crystalline dust species are not useful for reproducing the observed SED. The best fit model requires the largest stellar luminosity ( $47 L_{sun}$ ),  $\chi_{cg}$  (5.5), and rim height ( $H_{rim} = 0.1$  AU), which imply that the dust disk is the most flared and thickest among all of the sample stars.

HD 100546, which has the largest crystalline dust content (26%), shows emission features due to various crystalline dust species (forsterite, enstatite, water-ice, and corundum). We were not able to reproduce the wavelength range 3–8  $\mu\text{m}$ , which is dominated by the PAH features. The object shows prominent crystalline forsterite features at 19.5, 23.5, 27.5, and 33.5  $\mu\text{m}$ , but the best fit model produces much more prominent features. This could be because the forsterite grains exist in a separate cold outer dust component (about 100K) (Suh 2011), but the CGPLUS model can consider only a single disk component. This object requires the largest disk size ( $R_{out} = 600$  AU) among all the sample YSOs. Unlike the other HAB stars, the best fit model uses a relatively small  $\chi_{cg}$  (1.2) and rim height ( $H_{rim} = 0.029$  AU).

For HD 144432, the model uses various crystalline dust species (forsterite, enstatite, and corundum) as well as silicate (80%) and AMC. The crystalline dust makes a minor improvement in the model fit.

For HD 150193, the best fit model uses crystalline olivine (10%) as well as silicate (85%) and AMC (5%). The crystalline olivine produces a slightly better fit in the 9–30  $\mu\text{m}$  range.

We find that the theoretical model, CGPLUS, is useful for investigating the overall physical properties of the disk around the central star, even though it uses a single dust component of the disk geometry ignoring other dust disk or shell components (see Tables 1 and 2). The model parameters for the central star for the TTS stars are:  $M_{star} = 0.04\text{--}0.3 M_{sun}$ ,  $L_{star} = 0.13\text{--}1.5 L_{sun}$ , and  $T_{eff} = 2,600\text{--}3,500\text{K}$ . The parameters for the HAB stars are  $M_{star} = 2.2\text{--}2.6 M_{sun}$ ,  $L_{star} = 32\text{--}47 L_{sun}$ , and  $T_{eff} = 8,000\text{--}11,000\text{K}$ . Generally, the model requires a higher mass, luminosity, and temperature for the central star for the HAB stars than those for the CTT stars.

The model parameters for the dust disk for TTS stars are:  $R_{out} = 1.5\text{--}30$  AU,  $M_{disk} = 3.0 \times 10^{-4}\text{--}1.0 \times 10^{-2} M_{sun}$ ,  $\chi_{cg} = 1.8\text{--}3.5$ , and  $H_{rim} = 0.014\text{--}0.034$  AU. Those for HAB stars are:  $R_{out} = 10\text{--}600$  AU,  $M_{disk} = 1.010\text{--}2\text{--}5.010\text{--}2 M_{sun}$ ,  $\chi_{cg} = 1.2\text{--}5.5$ , and  $H_{rim} = 0.029\text{--}0.10$  AU. The outer radius, total mass, thickness, and

rim height of the dust disk for the HAB stars are generally larger than those for the CTT stars.

It is possible that the variety of the model parameters of the dust disk is not due to the different intrinsic property of the single central star, whether it is a CTT or a HAB star. Even though we have assumed that the central object is a single star for this work, it is believed that a major portion of the YSOs are binary and multiple systems, and these systems have significant dynamical effects on the structure of the dust disk (e.g., Bouwman et al. 2006; Hartmann 2009). The disk shapes for the sample YSOs could be significantly influenced by the binarity of the central object.

There could be three possible reasons for the unavoidable discrepancies between the theoretical and the observed SEDs. First, we may have not used some dust species that are present in the disks of the YSOs. Second, the dust opacity functions used in this work may need to be improved. Finally, the model for a single dust disk component used for this work could be too simple to reproduce all of the observed features.

## 5. DISCUSSION

Because emission features of crystalline dust grains are conspicuous, a small content (about 5-26%) can be easily observed (see Figs. 1 and 2). The crystalline grains can also improve the model fit in a wide spectral range for most objects. It is known that crystalline silicates are essentially missing from the interstellar medium, but they are abundant in many YSOs and solar system comets (e.g., Juhász et al. 2010; Suh 2014). Though the annealing crystallization mechanism suggested by Fabian et al. (2000) requires a high temperature (about 1,000K), other mechanisms that do not require a high temperature have also been suggested by various authors (SK2011). For most sample stars, we find that the dust temperature is low for a significant portion of the crystalline grains because the temperature of the outer regions of the disk is quite low ( $T_{out} = 83-460K$ ) (see Table 2). It is known that low temperature crystalline dust grains can effectively produce the prominent crystalline dust features for the sample stars (SK2011). Therefore, we expect that a significant portion of the crystalline dust grains that produce the crystalline dust features would be in low temperature regions of the disk.

SK2011 used a radiative transfer model for multiple isothermal circumstellar dust shells to reproduce the SEDs of the YSOs. Generally, the multiple dust shell model reproduced the observed SEDs of the YSOs better than the single dust disk model used for this work. Because the

basic schemes of the two models (SK2011 and this work) are totally different, the dust compositions derived from the two models cannot be directly compared. Furthermore, SK2011 did not use the crystalline olivine dust that produces peaks at some wavelengths similar to those for crystalline corundum or forsterite (see Fig. 3). Therefore, even though the overall dust compositions appear fairly similar, the detailed dust compositions derived from the two models show some discrepancies.

The isothermal multiple dust shell model used by SK2011 would be more useful for identifying the dust composition because it reproduces the observed SEDs much better without providing detailed physical properties (density distributions) of the dust envelopes. In contrast, the single dust disk model (CGPLUS) used in this work makes reasonable estimations of the physical properties (the detailed density distribution and mass) of the dust disk. The model parameters derived in this work would be useful for preparing initial model parameters of a more complicated radiative transfer model, which can thoroughly consider multiple dust disk and shell components (e.g., Suh 2016).

## 6. CONCLUSIONS

To reproduce the SEDs of the YSOs, we have used a radiative transfer model for the irradiated circumstellar dust disk with various shapes and many dust species. For eight sample objects of the CTT and HAB stars, we have compared the theoretical model results with the observed SEDs described by the Spitzer and ISO spectral data. We have found that crystalline dust as well as amorphous dust in the disk can reproduce the observed SEDs fairly well for most of the sample stars.

We have presented the best fit model parameters of the dust disk for the eight sample stars after comparing the theoretical model SEDs with the observed SEDs. We have found that the model requires a higher mass, luminosity, and temperature for the central star for the HAB stars than for the CTT stars. Generally, the outer radius, the total mass, the thickness, and the rim size of the dust disk for the HAB stars are larger than those for the CTT stars. These disk model parameters could be significantly influenced by the binarity of the central object.

Because a major portion of the YSOs are believed to be binary and multiple systems, we may need to consider their dynamic effects in modeling the circumstellar dust envelopes around the YSOs. We expect that the model parameters of the dust disks obtained in this work would be useful for further investigations using a radiative transfer

model that can consider multiple dust disk and shell components.

## ACKNOWLEDGMENTS

This work was supported by the research grant of the Chungbuk National University in 2014. This research was supported by Basic Science Research Program through the National Research Foundation of Korea (NRF) funded by the Ministry of Science, ICT & Future Planning (NRF-2013R1A1A2057841).

## REFERENCES

- Bertie JE, Labbé HJ, Whalley E, Absorptivity of ice in the range 4000-30 cm<sup>-1</sup>, *J. Chem. Phys.* 50, 4501-4520 (1969). <http://dx.doi.org/10.1063/1.1670922>
- Bertout C, T Tauri stars: wild as dust, *Annu. Rev. Astron. Astrophys.* 27, 351-395 (1989). <http://dx.doi.org/10.1146/annurev.aa.27.090189.002031>
- Bohren CF, Huffman DR, Absorption and scattering of light by small particles (Wiley, New York, 1983).
- Bouwman J, Lawson WA, Dominik C, Feigelson ED, Henning Th, et al., Binarity as a key factor in protoplanetary disk evolution: *Spitzer* disk census of the  $\eta$  Chamaeleontis Cluster, *Astrophys. J.* 653, L57-L60 (2006). <http://dx.doi.org/10.1086/510365>
- Bouwman J, Henning Th, Hillenbrand LA, Meyer MR, Pascucci I, et al., The formation and evolution of planetary systems: grain growth and chemical processing of dust in T Tauri systems, *Astrophys. J.* 683, 479-498 (2008). <http://dx.doi.org/10.1086/587793>
- Cambrésy L, Copet E, Epchtein N, de Batz B, Borsenberger J, et al., New young stellar object candidates in the Chamaeleon I molecular cloud discovered by DENIS, *Astron. Astrophys.* 338, 977-987 (1998).
- Chiang EI, Goldreich P, Spectral energy distributions of T Tauri stars with passive circumstellar disks, *Astrophys. J.* 490, 368-376 (1997). <http://dx.doi.org/10.1086/304869>
- Dullemond CP, Dominik C, Natta A, Passive irradiated circumstellar disks with an inner hole, *Astrophys. J.* 560, 957-969 (2001). <http://dx.doi.org/10.1086/323057>
- Fabian D, Jäger C, Henning Th, Dorschner J, Mutschke H, Steps toward interstellar silicate mineralogy. V. Thermal evolution of amorphous magnesium silicates and silica, *Astron. Astrophys.* 364, 282-292 (2000).
- Fabian D, Henning T, Jäger C, Mutschke H, Dorschner J, et al., Steps toward interstellar silicate mineralogy VI. Dependence of crystalline olivine IR spectra on iron content and particle shape, *Astron. Astrophys.* 378, 228-238 (2001). <http://dx.doi.org/10.1051/0004-6361:20011196>
- Hartmann L, Accretion processes in star formation (Cambridge University Press, New York, 2009).
- Ivezić A, Elitzur M, Self-similarity and scaling behaviour of infrared emission from radiatively heated dust. I. Theory, *Mon. Not. Roy. Astron. Soc.* 287, 799-811 (1997).
- Jäger C, Molster FJ, Dorschner J, Henning Th, Mutschke H, et al., Steps toward interstellar silicate mineralogy. IV. The crystalline revolution, *Astron. Astrophys.* 339, 904-916 (1998).
- Juhász A, Bouwman J, Henning Th, Acke B, van den Ancker ME, et al., Dust evolution in protoplanetary disks around Herbig Ae/Be stars-the *Spitzer* view, *Astrophys. J.* 721, 431-455 (2010). <http://dx.doi.org/10.1088/0004-637x/721/1/431>
- Lawson WA, Crause LA, Mamajek EE, Feigelson ED, The  $\eta$  Chamaeleontis cluster: photometric study of the ROSAT-detected weak-lined T Tauri stars, *Mon. Not. Roy. Astron. Soc.* 321, 57-66 (2001). <http://dx.doi.org/10.1046/j.1365-8711.2001.03967.x>
- Luhman KL, Allen LE, Allen PR, Gutermuth RA, Hartmann L, et al., The disk population of the Chamaeleon I star-forming region, *Astrophys. J.* 675, 1375-1406 (2008). <http://dx.doi.org/10.1086/527347>
- Malfait K, Bogaert E, Waelkens C, An ultraviolet, optical and infrared study of Herbig Ae/Be Stars, *Astron. Astrophys.* 331, 211-223 (1998).
- Meeus G, Waters LBFM, Bouwman J, van den Ancker ME, Waelkens C, et al., ISO spectroscopy of circumstellar dust in 14 Herbig Ae/Be systems: towards an understanding of dust processing, *Astron. Astrophys.* 365, 476-490 (2001). <http://dx.doi.org/10.1051/0004-6361:20000144>
- Megeath ST, Hartmann L, Luhman KL, Fazio GG, *Spitzer*/IRAC photometry of the  $\eta$  Chamaeleontis association, *Astrophys. J.* 634, L113-L116 (2005). <http://dx.doi.org/10.1086/498503>
- Mundt R, Bastian U, UVB photometry of Young emission-line objects, *Astron. Astrophys. Suppl. Ser.* 39, 245-250 (1980).
- Murakami H, Baba H, Barthel P, Clements DL, Cohen M, et al., The infrared astronomical mission AKARI, *Publ. Astron. Soc. Jpn.* 59, S369-S376 (2007). <http://dx.doi.org/10.1093/pasj/59.sp2.S369>
- Olofsson J, Augereau JC, van Dishoeck EF, Merín B, Lahuis F, et al., C2D *Spitzer*-IRS spectra of disks around T Tauri stars IV. Crystalline silicates, *Astron. Astrophys.* 507, 327-345 (2009). <http://dx.doi.org/10.1051/0004-6361/200912062>
- Olofsson J, Augereau JC, van Dishoeck EF, Merín B, Grosso N, et al., C2D *Spitzer*-IRS spectra of disks around T Tauri stars. V. Spectral decomposition, *Astron. Astrophys.* 520, A39 (2010). <http://dx.doi.org/10.1051/0004-6361/200913909>

- Shevchenko VS, Herbst W, The search for rotational modulation of T Tauri stars in the Ophiuchus dark cloud, *Astron. J.* 116, 1419-1431 (1998). <http://dx.doi.org/10.1086/300496>
- Sicilia-Aguilar A, Bouwman J, Juhasz A, Henning Th, Roccatagliata V, et al., The long-lived disks in the  $\eta$  Chamaeleontis cluster, *Astrophys. J.* 701, 1188-1203 (2009). <http://dx.doi.org/10.1088/0004-637x/701/2/1188>
- Simon M, Ghez AM, Leinert Ch, Cassar L, Chen WP, et al., A lunar occultation and direct imaging survey of multiplicity in the Ophiuchus and Taurus star-forming regions, *Astrophys. J.* 443, 625-637 (1995). <http://dx.doi.org/10.1086/175554>
- Skrutskie MF, Cutri RM, Stiening R, Weinberg MD, Schneider S, et al., The Two Micron All Sky Survey (2MASS), *Astron. J.* 131, 1163-1183 (2006). <http://dx.doi.org/10.1086/498708>
- Spangler C, Sargent AI, Silverstone MD, Becklin EE, Zuckerman B, Dusty debris around solar-type stars: temporal disk evolution, *Astrophys. J.* 555, 932-944 (2001). <http://dx.doi.org/10.1086/321490>
- Suh KW, Optical properties of the silicate dust grains in the envelopes around asymptotic giant branch stars, *Mon. Not. Roy. Astron. Soc.* 304, 389-405 (1999). <http://dx.doi.org/10.1046/j.1365-8711.1999.02317.x>
- Suh KW, Optical properties of the carbon dust grains in the envelopes around asymptotic giant branch stars, *Mon. Not. Roy. Astron. Soc.* 315, 740-750 (2000). <http://dx.doi.org/10.1046/j.1365-8711.2000.03482.x>
- Suh KW, Dust around Herbig Ae/Be stars, *J. Kor. Astron. Soc.* 44, 13-21 (2011). <http://dx.doi.org/10.5303/jkas.2011.44.1.13>
- Suh KW, Astrophysics of dusty stellar winds from AGB stars, *J. Kor. Astron. Soc.* 47, 219-233 (2014). <http://dx.doi.org/10.5303/JKAS.2014.47.6.219>
- Suh KW, A model for the dust envelope of the silicate carbon star IRAS 09425-6040, *Astrophys. J.* 819, 61-72 (2016). <http://dx.doi.org/10.3847/0004-637X/819/1/61>
- Suh KW, Kwon YJ, Dust around T Tauri stars, *J. Astron. Space Sci.* 28, 253-260 (2011). <http://dx.doi.org/10.5140/JASS.2011.28.4.253>
- Tamanai A, Mutschke H, Blum J, Posch Th, Koike C, et al., Morphological effects on IR band profiles - Experimental spectroscopic analysis with application to observed spectra of oxygen-rich AGB stars, *Astron. Astrophys.* 501, 251-267 (2009). <http://dx.doi.org/10.1051/0004-6361/200911614>
- Waters LBFM, Waelkens C, Herbig Ae/Be stars, *Annu. Rev. Astron. Astrophys.* 36, 233-266 (1998). <http://dx.doi.org/10.1146/annurev.astro.36.1.233>
- Whitney BA, Wood K, Bjorkman JE, Wolff MJ, Two-dimensional radiative transfer in protostellar envelopes. I. Effects of geometry on class I sources, *Astrophys. J.* 591, 1049-1063 (2003). <http://dx.doi.org/10.1086/375415>
- Wright EL, Eisenhardt PRM, Mainzer AK, Ressler ME, Cutri RM, et al., The Wide-field Infrared Survey Explorer (WISE): mission description and initial on-orbit performance, *Astron. J.* 140, 1868-1881 (2010). <http://dx.doi.org/10.1088/0004-6256/140/6/1868>